DOI: 10.1111/cgf.13961
Eurographics Conference on Visualization (EuroVis) 2020
M. Gleicher, T. Landesberger von Antburg, and I. Viola
(Guest Editors)

Volume 39 (2020), Number 3

Representative Isovalue Detection and Isosurface Segmentation Using Novel Isosurface Measures

Cuilan Wang

School of Science & Technology, Georgia Gwinnett College, USA

Abstract

Interval volume is the volume of the region between two isosurfaces. This paper proposes a novel measure, called VOA measure, that is computed based on interval volume and isosurface area. This measure represents the rate of change of distance between isosurfaces with respect to isovalue. It can be used to detect representative isovalues of the dataset since two isosurfaces near material boundaries tend to be much closer to each other than two isosurfaces in material interiors, assuming they have the same isovalue difference. For the same isosurface, some portion of it may pass through the boundary of two materials and some portion of it may pass through the interior of a material. To separate the portions of an isosurface that represent different features of the dataset, another novel isosurface measure is introduced. This measure is calculated based on the Euclidean distance of individual sample points on two isosurfaces. The effectiveness of the two new measures in detecting significant isovalues and segmenting isosurfaces are demonstrated in the paper.

1. Introduction

Isosurface visualization, which involves visualizing surfaces of constant value in volumetric datasets, is an important visualization technique for exploring data and discovering knowledge. The best known isosurface extraction algorithm is Marching Cubes (MC) [LC87]. It produces a triangular mesh to approximate the isosurface for a scalar, rectilinear volumetric dataset. Over the years, many algorithms have been developed to improve the topological correctness, accuracy, and performance of MC [NY06, Wen13]. However, even with the isosurface extraction algorithms, it can still be a challenge to clearly visualize the structures in a volumetric dataset with isosurfaces. This is because in a volume dataset different structures are often represented by isosurfaces with different isovalues. Therefore, providing the guidance in choosing representative isovalues is very important in isosurface visualization.

The first contribution of this paper is a new measure, called the VOA (i.e., volume over area) measure, which can be used to detect representative isovalues. Interval volume is the volume of the region between two isosurfaces [Guo95, FMS95]. Here, this region is called the interval volume region (i.e., interval region for short). The ratio of the interval volume over the average area of the two isosurfaces that enclose the interval volume region is more meaningful than interval volume since it can remove the size factor of isosurface, which affects interval volume. This ratio approximates the average distance between two isosurfaces. The VOA measure further normalizes the ratio by the isovalue difference of the two isosurfaces. Thus, VOA represents the rate of change of the distance between two isosurfaces with respect to isovalue. Since near material boundaries two isosurfaces tend to be much closer to each other than two isosurfaces in material interiors, assuming they have the same isovalue difference, this measure can be used to identify representative isovalues that correspond to different structures. VOA is also similar to mean gradient magnitude integrated over an isosurface (i.e., mean gradient for short), but has an inverse relationship with mean gradient. Results in this paper show that VOA is more robust than mean gradient in detecting significant isovalues.

Separating the portions of an isosurface that represent different structures can aid in learning structural information about the dataset and rendering true features of the dataset. Also, the produced triangular mesh isosurface provides an explicit geometric representation of the feature of interest which can be used for future modeling, numerical simulations, etc. This is not provided by direct volume rendering techniques [Kni02].

The second contribution of the paper is a novel segmentation method that uses a local distance-based measure to segment the portions of an isosurface that represent the different structures of the dataset. The measure is calculated based on the Euclidean distance of individual sample points on two isosurfaces. The new method is designed based on the observation that at material boundaries two isosurfaces with large isovalue difference can have very small distance between each other, while they may be far away from each other at other locations.

The paper is organized as follows. In Section 2, related work is described. In Section 3, the VOA measure is introduced. In Section 4, the isosurface segmentation method is presented. The paper is concluded in Section 5.

2. Related Work

2.1. Measuring Interval Volume

Some methods have been developed to measure the interval volume [Wen13]. The histogram method counts the number of grid vertices with each scalar value σ in a scalar grid, which represents the frequency of the scalar value σ in the grid. Let $g(\sigma)$ denote this frequency. The histogram can be represented by a bar graph or a polygonal line with vertices $(\sigma, g(\sigma))$. For scalar regular-grid volumetric datasets, where each grid cell is a unit cube, as the sampling resolution increases, the histogram has been proven to converge to a sequence of the interval volume measures where each bin of the histogram corresponds to the isovalue interval of an interval volume measure in the sequence [DCM13]. Therefore, histogram can be used to approximate interval volume measures.

Scheidegger et al. proposed a measure, called weighted isosurface area, that approximates the interval volume distribution by taking the area of the isosurface for each cell and multiplying it by the inverse of gradient magnitude, which is approximated by cell span [SSD*08]. This is like replacing the isosurface with a thin shell of non-uniform thickness and computing the volume of this thin shell. They also proposed to use cheap alternatives, such as active edge count, active cube count, and, triangle count, to approximate the isosurface area in their formula. When active cube count is used as the alternative, the measure is called the weighted cube count. However, this method doesn't consider the existence of homogenous cells (i.e., all 8 vertices of the cell have the same value) which do not intersect the isosurface.

Duffy et al. made an adjustment to Scheidegger et al.'s weighted isosurface area measure by including the volume of the cells that are entirely within the interval region. In this paper, this measure is called adjusted weighted isosurface area. However, when this measure is used to approximate the interval volume measure, it doesn't guarantee the sum of the measures for all isovalue intervals equal to the volume of the whole dataset, which it should be for the true interval volume values. This is mainly because the inverse cube span is only a very coarse approximation of gradient magnitude. Duffy et al. also modified Scheidegger et al.'s weighted cell count measure to include the volume of the cells that are entirely inside the interval region. Here, this measure is called adjusted weighted cell count. This measure guarantees that the total of all the interval volume measures equal to the volume of the dataset.

2.2. Selecting Features of Interest

Histogram has been be used for detecting significant isovalues that represent the important features in a volumetric dataset. However, many datasets' sampling resolution is not high enough for the histogram method to produce smooth and useful results. Histograms are often noisy, which makes it difficult to detect representative isovalues. Other methods mentioned in Section 2.1 that produce approximations to interval volumes can also be used for identifying significant isovalues.

Another category of methods that have been used for selecting features of interest is to use local properties of a dataset, such as first and second derivatives. Kindlmann [Kin99] demonstrated that plotting the gradient magnitude and data value of each vertex in a volumetric dataset as a point generates a scatterplot diagram. In such a diagram, boundary regions are shown as arches. Kniss et al. [KKH02] extended this idea to develop a direct manipulation interface that can be used for designing good transfer functions for direct volume rendering. Tenginakai et al. [TLM01] proposed the model-independent statistical methods based on central moments of data that can be used to determine the salient isosurfaces at material boundaries. Pekar et al. [PWB01] suggested that total gradient and mean gradient computed using the Laplacian can guide the detection of representative isovalues.

Khoury and Wenger [KW10] demonstrated that the isosurface fractal dimension is corelated with noise in the isosurface. Plotting the fractal dimension against isovalues provides information about the isosurfaces in the dataset. Bruckner and Möller calculated similarities between individual isosurfaces in a volumetric dataset and use this global metric to develop an automatic method for identifying representative isovalues [BM10].

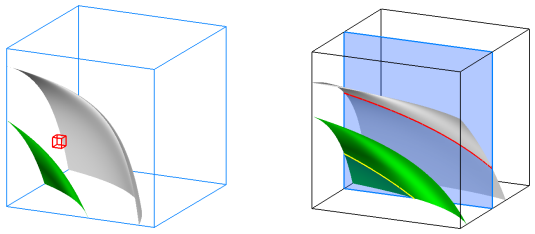

(a) subdividing method (b) slicing method

Figure 1: *Illustration of the two methods for accurate computation of interval volume.*

2.3. Accurate Computation of Interval Volume

In a recent research work [Wan19], two new methods, called the subdivision method and the slicing method, that can compute interval volume measures with very high accuracy are introduced. For these two methods, the input datasets are scalar regular-grid volumetric datasets and the interior of the grid cell is modeled by trilinear interpolation.

The subdividing method recursively subdivides each grid cube into 8 equal-sized subcubes until certain termination conditions are met or the subdivision limit is reached. Then, each subcube's contribution to the interval volume is determined. Summing up their contributions yields the cube's contribution to the interval volume. The interval volume for the whole dataset is the sum of all cubes' contribution to the interval volume. This idea is illustrated in Figure 1 (a), where the small red subcube is inside the interval region between the gray and green isosurfaces, thus, its volume contributes to the interval volume measure.

In this method, if the data range of a subcube doesn't intersect with the isovalue range of the interval volume, it doesn't need to be further subdivided. When the subdivsion limit is reached, a final subcube's contribution to the interval volume measure is approximated using a method similar to Duffy et al.'s adjusted weighted

cube count method [DCM13]. In [DCM13], Duffy et al. gave the proof of convergence of the measures generated by their adjusted weighted cube count method to the true interval volume measures as the sampling rate of the volume dataset increases based on Riemann integration. Similar Riemann proof can be easily extended to prove that the measures computed by the subdividing method converge to the true interval volume measures assuming the underlying function inside the grid cube is defined by trilinear interpolation. This is because the subdividing strategy is just a way to increase the sampling rate and the method's early termination condition is only used to save sampling in the subcubes that are entirely inside or outside the interval region.

In the slicing method, each cube is evenly sliced along a major axis. The cross-sectional area of the interval region on each slice is calculated analytically. This is based on the fact that the intersection of the trilinear interpolation isosurface with a slice is a hyperbola, which represents the isocontour of the bilinear interpolation on the slice. Then, a numerical approach that is similar to integrating areas to find volume is applied to generate the interval volume inside the cube. Assuming that the cross-sectional area between two adjacent slices is a constant, the interval volume inside the cube can be approximated by integrating the cross-sectional area multiplied by the distance between two adjacent slices.

The main idea of this method is illustrated in Figure 1 (b). Here, the interval region is the region between the green and gray isosurfaces. The intersections of the slice (light blue and semi-transparent) with the green and gray isosurfaces are shown as the yellow and red curves, respectively. The area between the yellow and red curves is the cross section of the interval region on the slice.

In the subdividing method, the higher the subdivision depth, the more accurate the results generated. In the slicing Method, the number of slices that a cube is sliced into determines the precision of the method. Experimental results in [Wan19] show that the interval volume measures generated by the subdividing and slicing methods converge to the same set of values. Both methods are able to produce very accurate internal volume measures when the underlying function inside the grid cell is defined by trilinear interpolation. Results also show that the slicing method takes much less time to converge than the subdividing method since the cross-sectional area of the interval region is computed analytically. In this paper, the slicing method with 32 slices is used to compute the interval volume.

3. New Metric for Selecting Representative Isovalues

3.1. The VOA (Volume Over Area) Measure

In a volumetric dataset, materials boundaries usually are narrow and have large data value variation, while materials interiors usually are wide and have small data value variation. Thus, at material boundaries two isosurfaces tend to be closer to each other than two isosurfaces in material interiors, assuming they have the same isovalue difference. Therefore, the rate of change of distance between two isosurfaces with respect to isovalue can be used to detect representative isovalues.

The interval volume between two isosurfaces are affected by both the distance between the two isosurfaces and the isosurface area. Dividing the interval volume by the average area of the two isosurfaces that enclose the interval volume region gives an approximation of the average distance between the two isosurfaces. The VOA measure computes the rate of change of this distance with respect to isovalue. It is calculated as

$$d_{VOA}(\sigma_1,\sigma_2) = \frac{V(\sigma_1,\sigma_2)}{(\frac{S(\sigma_1)+S(\sigma_2)}{2}) \times (\sigma_2-\sigma_1)} \tag{1}$$

where $V(\sigma_1,\sigma_2)$ is the interval volume between the two isosurfaces associated with isovalues σ_1 and σ_2, assume $\sigma_1 < \sigma_2$, and $S(\sigma)$ is the area of the isosurface with isovalue σ.

Let f be a scalar function defined in the domain of the volumetric dataset. Function $f^{-1}(\sigma)$ defines an isosurface of f with isovalue σ. In [SSD*08], based on Federer's Co-Area formula [Mor16], Scheidegger et al. showed that the interval volume measure can be computed as:

$$\begin{aligned} V(\sigma_1,\sigma_2) &= \int_{\sigma_1}^{\sigma_2} \int_{f^{-1}(\sigma)} \frac{1}{|\nabla f|} dS d\sigma \\ &= \int_{\sigma_1}^{\sigma_2} C(\sigma) d\sigma, \end{aligned} \tag{2}$$

where $C(\sigma)$ is the interval volume distribution function at isovalue σ and it is equal to:

$$C(\sigma) = \int_{f^{-1}(\sigma)} \frac{1}{|\nabla f|} dS \tag{3}$$

Here, $|\nabla f|$ is the gradient magnitude of function f, which represents the rate of change of isovalue with respect to distance at a specific point. Thus, the inverse gradient magnitude, $\frac{1}{|\nabla f|}$, represents the rate of change of distance between isosurfaces with respect to isovalue at a specific point.

Let $\sigma' \in (\sigma, \sigma+\Delta\sigma)$. If both $S(\sigma')$ and $C(\sigma')$ are very constant within the range of $(\sigma, \sigma+\Delta\sigma)$, which is usually true if $\Delta\sigma$ is very small, then $V(\sigma, \sigma+\Delta\sigma)$ can be approximated by

$$V(\sigma, \sigma+\Delta\sigma) \approx C(\sigma)\Delta\sigma, \tag{4}$$

and $d_{VOA}(\sigma, \sigma+\Delta\sigma)$ can be approximated by

$$d_{VOA}(\sigma, \sigma+\Delta\sigma) \approx \frac{C(\sigma)}{S(\sigma)}, \tag{5}$$

Therefore, the VOA measure approximates the integral of the inverse gradient magnitude over the isosurface divided by the area of the isosurface.

3.2. Comparison with Mean Gradient

The mean gradient measure proposed in [PWB01] is the average gradient magnitude over the isosurface. Equation 5 shows that VOA approximates the average inverse gradient magnitude over the isosurface, thus, it is inversely corelated with mean gradient. However, VOA and mean gradient are not exact inverse of each other, since the average inverse gradient magnitude is not the inverse average gradient magnitude. There can be obvious differences between one measure and the inverse of the other, especially when the gradient magnitudes over an isosurface have a relatively large variation. The VOA measure provides another way to identify significant isovalues.

The mean gradient can be computed using a Laplacian based method [PWB01], which requires the computation of the Laplace values at grid vertices. The Laplace value at a grid vertex is usually computed using the vertex's 6 neighboring vertexes' values based on the second central difference method. However, this method doesn't produce good results if the isosurface is not closed [Wen13]. This is a big problem if mean gradient needs to be used for local regions of the dataset, where the isosurfaces are usually not closed.

In some research work [SSD*08, DCM13, Wen13], the gradient magnitude for a cube region is approximated by the cube span, which is the difference between the largest and smallest vertex values of the cube [Wen13]. However, the cube span usually overestimates the gradient magnitude [SSD*08]. In the experiments reported in this paper, a method, called the cube center gradient method, is used to compute gradient magnitude. The method first uses bilinear interpolation on cube faces to compute the value of each cube face's center. Then, the difference between the values of opposite cube faces' centers is used as one component of the gradient vector at the cube center. Finally, the gradient magnitude is computed from this gradient vector. This method gives a better approximation of gradient magnitude for a cube region than the cube span method since it uses all 8 cube vertexes' values to compute the gradient magnitude, instead of only the largest and smallest vertex values of the cube.

The total gradient of an isosurface is the sum of the gradient magnitudes of all cubes that intersect the isosurface. The mean gradient is the total gradient divided by the area of the isosurface. Sometimes, the isosurface area is approximated by the number of cubes that intersect the isosurface [SSD*08]. When the cube center gradient method is used to compute the gradient magnitude and the active cube count is used for the isosurface area, what is doing to compute mean gradient essentially is that the gradient is sampled at the center of each cube that intersects the isosurface, and then all those cubes' sampled gradients' magnitudes are averaged.

However, for each cube, the gradient magnitude computed using the cube span or cube center gradient methods is fixed for the whole cube region. The gradient magnitude changes inside the cube may be missed. On the other hand, the VOA measure uses the interval volume measure, which considers the entire space between the two isosurfaces, not isolated samples. Also, the interval volume measure calculated using the slicing method can have high accuracy. Thus, VOA can have high accuracy in capturing the rate of change of distance between isosurfaces with respect to isovalue inside a cube. Therefore, the VOA plots can be smoother and more accurate for identifying significant isovalues than the mean gradient plots, especially for the low resolution datasets or local regions of a dataset.

3.3. Experimental Results

Let A_i, $M_{min} \leq i \leq M_{max}$, be the interval region associated with the isovalue range $[i-0.5, i+0.5)$, where i is an integer and $[M_{min}, M_{max}]$ be the rangle of isovalues for the VOA plot. In this paper, to generate the VOA plot, first, the interval volume is calculated using the slicing 32 method for each interval region A_i; then, the areas of two bounded isosurfaces of A_i (i.e., the isosurfaces with isovalues $i+0.5$ and $i-0.5$) are calculated; finally, the VOA measure is computed using Equation 1. To calculate the isosurface area for the VOA measure, the Marching Cubes algorithm is used to extract a triangular mesh to represent the isosurface. The sum of the areas of all triangles in the mesh gives an approximation of the isosurface area. Also, in order to compare, each measure reported in this section is normalized by its own sum over all isovalue intervals.

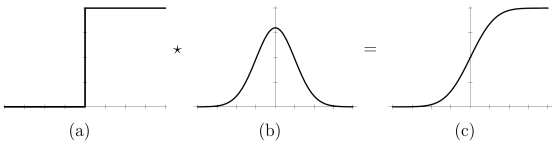

Figure 2: *The ideal boundary is represented with a step function (a). The step function is convolved with a Gaussian function (b), producing the blurred boundary function (c), which exhibits the shape of the $erf()$ function. (Adapted from [Kin99])*

3.3.1. Synthetic Dataset Experiments

Here, the VOA measure was tested with a synthetic dataset which contains two materials with isovalues 20 and 200. The high value material is inside a sphere with radius r centered at the volume center. The rest of the volume is occupied with the low value material. Thus, the ideal boundary between the two materials is a sphere. Along each radial direction of the sphere, a 1D Gaussian filter is implemented to blur the boundary between the two materials based on the boundary model given in [Kin99]. In this model, the ideal boundary function is represented by a step function (Figure 2 (a)). The Gaussian function (Figure 2 (b)) blurs the idea boundary. The resulting boundary curve (Figure 2 (c)) happens to be the integral of the Gaussian function, which is called the error function, notated $erf()$. The $erf()$ function is defined as

$$\begin{aligned} erf(x) &= \frac{1}{\sqrt{\pi}} \int_{-x}^{x} e^{-t^2} dt \\ &= \frac{2}{\sqrt{\pi}} \int_{0}^{x} e^{-t^2} dt. \end{aligned} \tag{6}$$

The boundary data value is given as a function of the position [Kin99]:

$$v = f(x) = v_{min} + (v_{max} - v_{min}) \frac{1 + erf(\frac{x}{\sigma\sqrt{2}})}{2}, \tag{7}$$

where v is the data value of a point, x is the distance of the point to the idea boundary, and v_{min} and v_{max} are the data values of the two materials on either side of the boundary. The parameter σ, which is the standard deviation of the Gaussian function, controls the thickness of the blurred boundary. When the sphere dataset is generated, first, each vertex's distance to the volume center is calculated; then, this distance subtracting by r gives the point's distance to the ideal boundary; next, its data value is computed using Equation 7.

The first derivative of f is given in [Kin99] as follows:

$$f'(x) = \frac{v_{max} - v_{min}}{\sigma\sqrt{2\pi}} exp(-\frac{x^2}{2\sigma^2}), \tag{8}$$

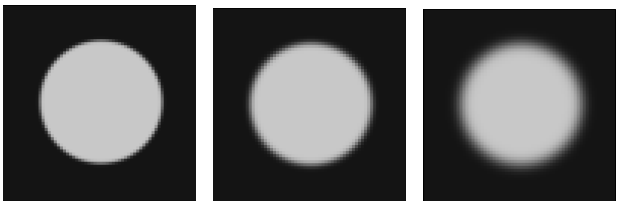

(a) $\sigma = 0.5$ (b) $\sigma = 1$ (c) $\sigma = 2$

Figure 3: *Cross-sections of the three sphere datasets with different* σ *values.*

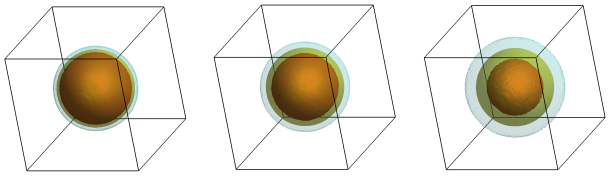

(a) $\sigma = 0.5$ (b) $\sigma = 1$ (c) $\sigma = 2$

Figure 4: *3D renderings of the three sphere datasets with different* σ *values.*

Since the sphere dataset is spherical symmetric, all the isosurfaces are concentric spheres. Thus, the gradient direction at a point is the direction of the radial line passing through the point and the gradient magnitude at the point is the first derivative of f. Therefore, all points with the same distance to the volume center have the same data value and same gradient magnitude. To convert the gradient magnitude from the function of the position to the function of the data value, points are densely sampled along the positive y axis. Given the y value of each sample point, its distance to the ideal boundary is $y - r$. The data value v and gradient magnitude f' of each sample point are calculated based on Equations 7 and 8 and are paired up. All pairs of (v, f') are plotted as points in a scatter plot to show the relationship between v and f'.

In the first experiment, the size of the dataset is $64 \times 64 \times 64$. The boundary sphere's radius, r, is 20. Three sphere datasets with the parameter σ in the Gaussian function being 0.5, 1, and 2 are generated. The cross-sections and 3D rendering of those sphere datasets are shown in Figures 3 and 4, respectively. The 3D rendering of the dataset is represented using the isosurfaces with isovalues 20.5, 110, and 199.5. The isosurface with isovalue 110 (half transparent and yellow) is where the idea boundary is. The region between the isosurface with isovalue 20.5 (half transparent and light blue) and the isosurface with isovalue 199.5 (brown) approximates the transition region between the two materials. The parameter σ controls the thickness of the boundary. Based on Equation 7, when the value of σ doubles, the width of the boundary also doubles. Let the side length of a grid cube in the dataset be 1. The distance between isosurfaces 20.5 and 199.5 is 2.8, 5.5, 11.1 for σ equals 0.5, 1, and 2, respectively.

Figure 5 compares the interval volume, isosurface area, and VOA measures for the synthetic sphere dataset with $\sigma = 1$. Results show that the plots of all three measures are smooth. As the isovalue

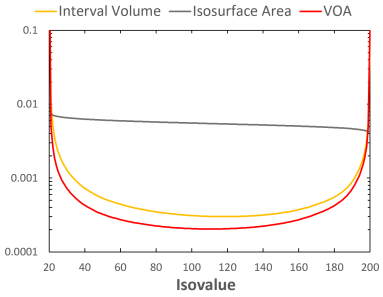

Figure 5: *Comparison of interval volume, isosurface area, and VOA for the sphere dataset with size* $64 \times 64 \times 64$ *and* $\sigma = 1$.

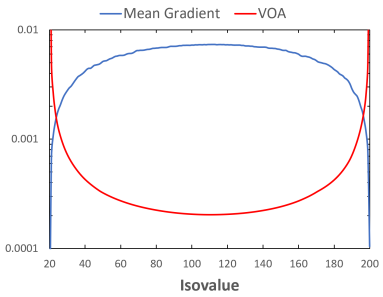

Figure 6: *Comparison of mean gradient and VOA for the sphere dataset with size* $64 \times 64 \times 64$ *and* $\sigma = 1$.

increases from 20 to 200, the isosurface area gradually decreases. This is because all isosurfaces in this dataset are spheres; as the isovalue increases, the radius of the isosurface spheres decreases, thus, the isosurface area decreases. The shape of the VOA plot is pretty symmetric about the center of the isovalue range, i.e., 110. However, the shape of the interval volume plot is not quite symmetric about the range center. The left half side is a little bit taller than the right half side affected by the isosurface area. The VOA plot also shows that the smallest VOA measure is at isovalue 110, which occurs at the middle of the boundary. As isovalue moves towards the two ends of the isovalue range, 20 and 200, which is also the values of the two materials, the VOA measure increases.

Figure 6 compares VOA and the mean gradient with gradients computed by the cube center gradient method for the sphere dataset with s = 1. Here, this mean gradient measure is called the sampled mean gradient (or mean gradient for short). Results show that the mean gradient and VOA are inverse of each other. In fact, because of the design of the sphere dataset, the mean gradient and VOA are exact inverse of each other. At the boundary of the two materials, the mean gradient is large, but VOA is small. In the material interiors, the mean gradient is small, while VOA is large. However, the results also show that the mean gradient plot is noisier than the VOA plot.

In the sphere dataset, the gradient magnitude is the same everywhere on an isosurface. Thus, the mean gradient is just the gradient magnitude at any point on the isosurface and can be calculated by Equation 8. This calculated mean gradient is the true mean gradient for the sphere dataset. Also, the reverse of VOA, which is

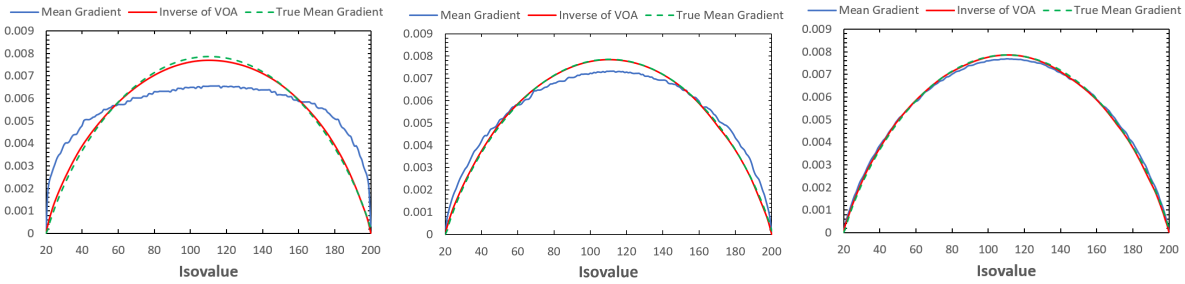

(a) $\sigma = 0.5$ (b) $\sigma = 1$ (c) $\sigma = 2$

Figure 7: *Comparison of mean gradient, inverse of VOA, and true mean gradient for the sphere dataset with size* $64 \times 64 \times 64$ *for three* σ *values.*

one divided by VOA, can be used to compare with the sampled mean gradient and true mean gradient to show the accuracy of VOA. Comparison of the sampled mean gradient, true mean gradient, and reverse of VOA for the three sphere datasets with σ being 0.5, 1, and 2 are shown in Figure 7 (a), (b), and (c), respectively. The results show that the reverse of VOA plot matches the true mean gradient plot better than the mean gradient plot, and the mean gradient plot is noisier than the reverse of VOA plot. In addition, as the σ value decreases, i.e., the volume of the boundary region decreases, the inverse of VOA plot is still very smooth and fits the true mean gradient plot well. On the other hand, the mean gradient plot gets noisier and doesn't match the true mean gradient plot well. This is because as the boundary region gets narrower, the number of gradient samples decreases. This makes the mean gradient unable to capture the gradient changes over the isovalue range well. Note that in the subfigures of Figure 7, as well as in Figures 9, 14, and 16 where mean gradient and the inverse of VOA are compared, the vertical axis is plotted on a linear scale, while the rest of figures in Section 3.3 that compare different measures have a log scale on the vertical axis.

In the second experiment, the $64 \times 64 \times 64$ sphere dataset with $r = 20$ and $\sigma = 0.5$, whose 3D rendering is shown in Figure 4 (a), was tested with another two different gird sizes: $32 \times 32 \times 32$ and $128 \times 128 \times 128$. In order to scale the idea boundary radius, r, and boundary region width proportionally to the side length of the volumetric dataset, when the side length doubles, r and σ both should double. For the $32 \times 32 \times 32$ dataset, $r = 10$, $\sigma = 0.25$. For the $128 \times 128 \times 128$ dataset, $r = 40$, $\sigma = 1$. The 3D renderings of all three datasets should look the same except that they are in different resolutions. Results show that when the grid size decreases, i.e., the data resolution decreases, the accuracy of both VOA and mean gradient decreases. However, mean gradient's accuracy degrades much more than VOA. Also, the mean gradient plot is much noisier than the VOA plot. For the $32 \times 32 \times 32$ dataset, the comparison of mean gradient and VOA is shown in Figure 8. This figure shows that for this dataset the mean gradient plot is noisy and flat, it doesn't capture the mean gradient changes over isovalues well, while the VOA plot is smooth and shows the changes of VOA over isovalues very well. The comparison of mean gradient, the reverse of VOA, and true mean gradient is shown in Figure 9.

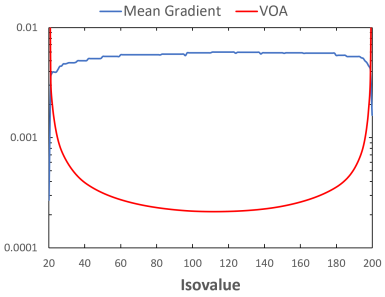

Figure 8: *Comparison of mean gradient and VOA for the sphere dataset with size* $32 \times 32 \times 32$ *and* $\sigma = 0.25$.

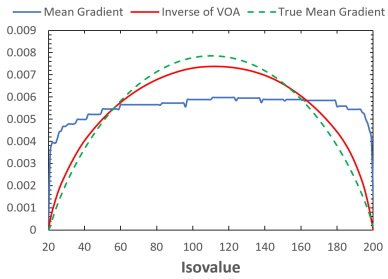

Figure 9: *Comparison of mean gradient, inverse of VOA, and true mean gradient for the sphere dataset with size* $32 \times 32 \times 32$ *and* $\sigma = 0.25$.

3.3.2. Real Dataset Experiments

3.3.2.1. Global Measures The results of testing the VOA measure with two CT-scan datasets are reported in Figures 10 and 11 for the engine and human head datasets, respectively. Subfigure (a) of each figure shows the comparison of three measures: interval volume, isosurface area, and VOA. Peaks in those plots usually indicate the materials themselves and troughs usually correspond to the boundaries between the materials. In isosurface visualization and direct volume rendering, material boundaries are usually the primary interest of rendering.

In Figure 10 (a), both interval volume and VOA clearly shows three peaks, which correspond to the background, the engine's

medium value material, and the engine's high value material. The trough between the first and second peak, which is called trough 1, and the trough between the second and third peaks, which is called trough 2, are associated with the boundaries between the materials. The isosurface area barely shows the second peak and completely misses the third peak. But it shows that the isosurface areas in trough 1 are larger than those in trough 2.

The VOA measure in trough 1 has about the same magnitude as it does in trough 2, while the interval volumes in these two troughs have obvious magnitude difference. This shows that VOA is a more meaningful measure than interval volume, because large interval volumes may cause by large isosurface areas, and vice versa. In this case, the smaller interval volume in trough 2 is due to the smaller isosurface area in trough 2.

In Figure 10 (a), the vertical dashed lines and the black dots correspond to the representative isovalues for the trough regions. The isosurfaces associated with the two representative isovalues are shown in (b) and (c). A rendering of the engine dataset combining these two isosurfaces are shown in (d). For global datasets, the VOA plots are often smooth, thus, local minimums usually can be used in choosing the representative isovalues. Here, approximated first derivative computed by the central difference method can be used to find the local minimums of the VOA plot. If the VOA plot is very noisy, then it needs to be smoothed first using some averaging filter to achieve good results.

For the human head dataset, Figure 11 (a) shows that the VOA measure indicates four peaks, while both the interval volume and isosurface area miss the last peak which is at about 235-255. The last peak corresponds to the tooth structure that has high data values. Since the teeth occupy much smaller space than other major structures, such as tissue and bone, both the isosurface area and interval volume have much smaller values for teeth than their values for other major structures. However, when the interval volume is divided by the isosurface area, it only keeps the distance information, while removes the size factor. Therefore, VOA is able to reveal important features that may not be detected by the other two measures. The three isosurfaces with the identified representative isovalues are shown in (b), (c), and (d). These three isosurfaces are combined in (e) to show their relative positions to each other.

For global measures, since the gradient is sampled at a large amount of grid cubes, the mean gradient plot is smooth and the mean gradient tends to be the inverse of VOA. Both measures are good at identifying global representative isovalues.

For the engine dataset, the VOA measure is computed for each of the isovalue interval $[i-0.5, i+0.5)$, $0 \leq i \leq 255$. The execution time to calculate all VOA measures is 108.6 seconds, in which 43.5 seconds are spent on computing interval volumes with the slicing 32 method and 65.1 seconds are spent on extracting isosurfaces with the Marching Cubes algorithm. The execution time to compute all mean gradients is 4.5 seconds. The time to compute VOA measures can be reduced by using less number of slices in the slicing method or using a faster isosurface extraction algorithm, such as Discretized Marching Cubes [MSS94]. For the human head dataset, the times to compute the VOA measures and mean gradients are 115.9 seconds and 4.4 seconds, respectively.

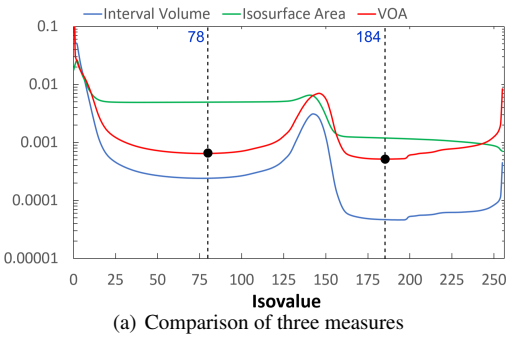

(a) Comparison of three measures

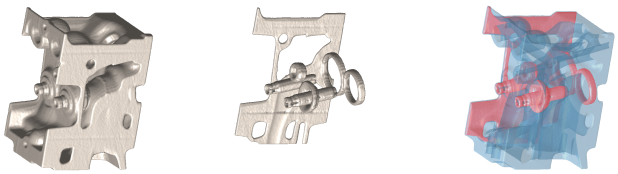

(b) Isovalue = 78 (c) Isovalue = 184 (d) Combined

Figure 10: *Representative isovalue selection for the engine dataset with the VOA measure. (a) shows the comparison of isosurface area, interval volume, and VOA. Isosurfaces with the presentative isovalues 78 and 184 are shown in (b) and (c). A combined rendering with both isosurfaces is displayed in (d).*

3.3.2.2. Local Measures In this set of experiments, the results of testing two local regions in the tooth dataset are reported. The size of each region is $6 \times 6 \times 6$ cubes. In Figure 12, the local regions are the regions inside black boxes; the local region in (a) contains the background and the dentin; the local region in (b) crosses the background and the enamel.

Figure 13 compares mean gradient and VOA for the neighborhood region in Figure 12 (a). Here, the vertical axis is plotted on a log scale. In this figure, the left and right peaks in the VOA plot indicate the background itself and the dentin itself, respectively; while the trough between the two peaks corresponds to the boundary between the two materials. This figure also shows that the mean gradient plot is noisier than the VOA plot. Also, the VOA plot has two obvious peaks that correspond to the representative isovalues for the two materials themselves in the local region, while the mean gradient plot doesn't have two obvious trough regions.

To demonstrate that the VOA plot is smoother than the mean gradient plot, Figure 14 compares the mean gradient and inverse of VOA for the local region in Figure 12 (a). Here, the vertical axis is plotted on a linear scale.

Similar results are obtained for the local region in Figure 12 (b). They are demonstrated in Figures 15 and 16.

For the background-dentin local region, the range of the isovalues is $[402, 851]$. The execution times to compute VOA measures and mean gradients are 2.2×10^{-2} and 2.0×10^{-4} seconds, respectively. The isovalue range for the background-enamel local region is $[413, 1262]$. For this local region, the times to compute VOA mea-

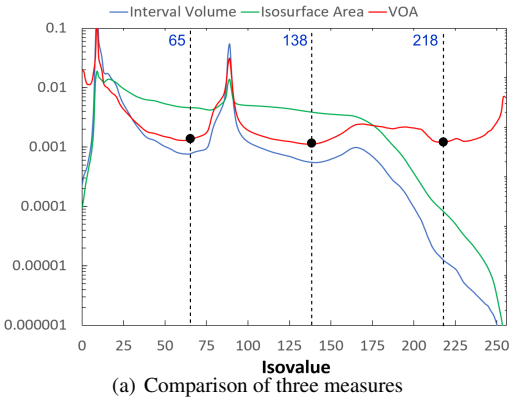

(a) Comparison of three measures

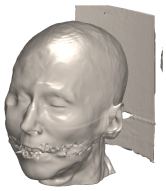

(b) Isovalue = 65

(c) Isovalue = 138

(d) Isovalue = 218

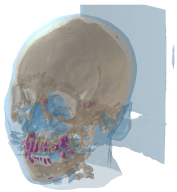

(e) Combined

Figure 11: *Representative isovalue selection for the human head dataset with the VOA measure.*

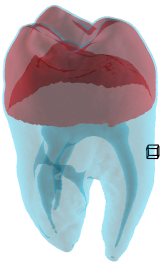

(a) background-dentin

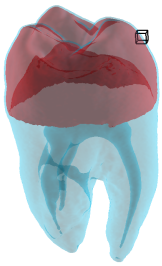

(b) background-enamel

Figure 12: *Two local regions in the tooth dataset.*

sures and mean gradients are 4.7×10^{-2} and 3.6×10^{-4} seconds, respectively. The background-enamel local region requires longer time to compute VOA measures than the background-dentin local region is because of its larger isovalue range. Results show that it takes longer time to compute VOA measures than mean gradients. The VOA measure trades the speed for accuracy and robustness.

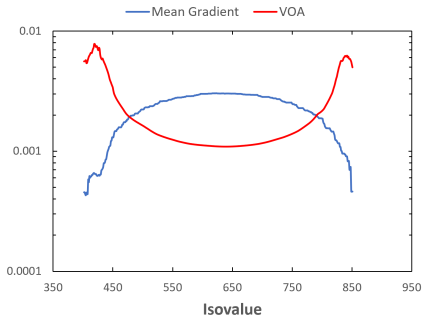

Figure 13: *Comparison of mean gradient and VOA for the dentin-background local region in Figure 12 (a).*

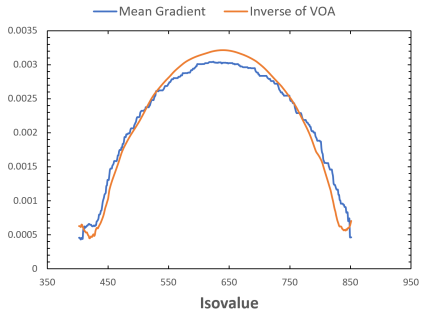

Figure 14: *Comparison of mean gradient and the inverse of VOA for the dentin-background local region in Figure 12 (a).*

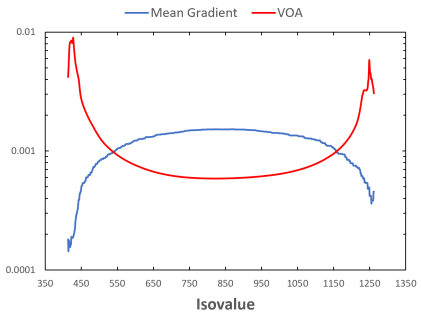

Figure 15: *Comparison of mean gradient and VOA for the enamel-background local region in Figure 12 (b).*

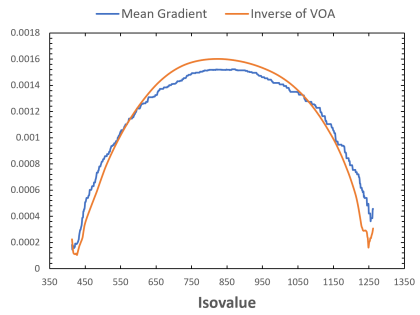

Figure 16: *Comparison of mean gradient and the inverse of VOA for the enamel-background local region in Figure 12 (b).*

4. Isosurface Segmentation with Distance-Based Measure

One isosurface may contain different features of the dataset. For example, if there are three materials M_1, M_2, and M_3 in a dataset, corresponding to data values σ_1, σ_2, and σ_3, respectively. Assume $\sigma_1 < \sigma_2 < \sigma_3$. If isovalue σ' is in between σ_1 and σ_2, then it must be in between σ_1 and σ_3 as well. Therefore, the isosurface with isovalue σ' not only passes through the boundary between M_1 and M_2, but also passes through the boundary between M_1 and M_3. In another example, for the isosurface with isovalue σ_2, it represents the material M_2. However, since it is in between σ_1 and σ_3, it also passes through the boundary between M_1 and M_3. The goal here is to separate the different features shown in one isosurface.

The isosurface segmentation method works well on isosurfaces associated with representative isovalues. Its main steps are given as follows. For an isosurface S with the representative isovalue σ, its reference isosurface $\hat{S}$ is first determined. To choose $\hat{S}$, the associated isovalue $\hat{\sigma}$ of $\hat{S}$ needs to be another representative isovalue. Also, S and $\hat{S}$ must have obvious differences in structure. Besides that, S and $\hat{S}$ must both pass a common material boundary so that they are very close to each other at that material boundary. Since there are obvious differences in their structures, they must be not very close at other locations. Next, at each cube that S intersects with, the shortest distance d from S to $\hat{S}$ is computed. A distance threshold ε is applied to separate S into two parts. One part is the part of S in the cubes where $d < \varepsilon$, which corresponds to the common material boundary shared by S and $\hat{S}$. The rest of S is the second part of S that does not pass that material boundary. The distance threshold d_t can be chosen if the thickness of the boundary is known from prior domain knowledge, or from a histogram plot of all those local shortness distances from S to $\hat{S}$ where peaks in the plot can be identified. Using a similar approach, the second part of S can be further segmented if another reference isosurface can be found.

It has been shown that in a two-dimensional histogram of data value and gradient magnitude, the boundaries between the materials are demonstrated as arches [Kin99]. In the upper right corner of Figure 17, the 2D histogram for the engine dataset is displayed as a scatterplot. A similar diagram is created to illustrate the data value of each material and the data value ranges for the materials boundaries. Such a diagram is shown in Figure 17 for the engine dataset. Here, this kind of diagrams are called isosurface segmentation diagrams. They can be used to guide the isosurface segmentation.

Next, the effectiveness of the segmentation method is demonstrated with the engine dataset. For this dataset, the isosurface with isovalue 78 is denoted as S_1' and the isosurface with isovalue 184 is denoted as S_2'. Here, isovalues 78 and 184 are the representative isovalues obtained using the VOA measure. The diagram in Figure 17 shows that S_1' passes through the air and medium value material boundary and the air and high value material boundary; S_2' crosses the air and high value material boundary and the medium value material and high value material boundary. Since S_1' and S_2' both cross the boundary between the air and high value material, they must be very close to each other at that boundary. Thus, the portion of S_1' that passes through that boundary must be much closer to S_2' than the rest of S_1'. Here, S_2' is used as a reference isosurface for segmenting S_1'.

To measure the local distance from isosurface S_1' to isosurface S_2',

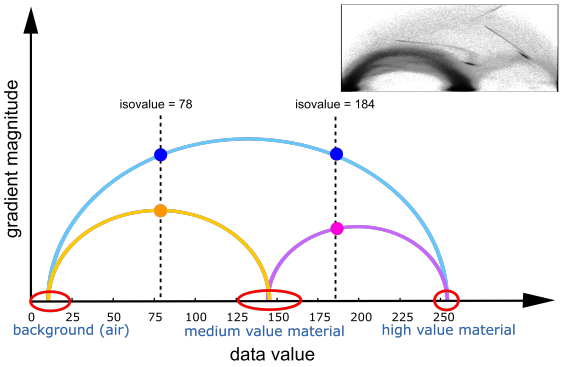

Figure 17: *Isosurface segmentation diagram for the engine dataset. The scatterplot is adapted from [Kin99].*

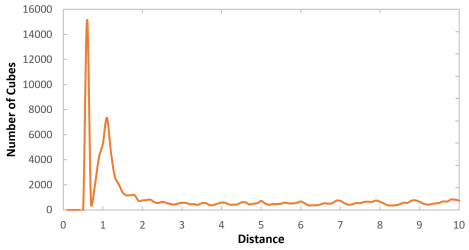

Figure 18: *Histogram of the local distances between the isosurface with isovalue 78 and the isosurface with isovalue 184 for the engine dataset.*

a distance-based measure is used. It is computed as follows. For a cube K_1 that S_1' passes through, its neighboring region is searched to find all cubes that intersect S_2'. For each intersected cube K_2, the distance between S_1' in K_1 and S_2' in K_2 is calculated. The smallest distance of all such distances is used as the distance of S_1' in K_1 to S_2'. To compute the distance of S_1' in K_1 to S_2' in K_2 (K_1 and K_2 can be the same cube), first, the Marching Cubes algorithm is applied to extract the triangular mesh that approximates the isosurface. The centroid of each triangle in the mesh is used as a sample point of the isosurface. Then, each sample point of S_1' in K_1 is paired up with each sample point of S_2' in K_2, and the Euclidean distance between each pair of the sample points is computed. The smallest distance of all pairs is used as the distance of S_1' in K_1 to S_2' in K_2. In fact, the mesh can be refined by subdividing the cube and applying Marching Cubes to subcubes. The more the cube is subdivided, the more sample points are obtained, thus, the more accurate the measure is.

Figure 18 shows a histogram of such distances of all cubes that isosurface S_1' intersects with to isosurface S_2'. It shows the number of cubes for each distance interval. In this diagram, there are two obvious peaks before 2. Here, the side length of a cube is 1. Those peaks are caused by the portion of S_1' that passes through the air and high value material boundary. With this kind of distance diagrams, a distance threshold ε can be chosen to segment the isosurface. Here, ε is set to 2.7.

When isosurface S_1' is segmented, the distance of S_1' to the reference isosurface S_2' is checked at each cube that intersects S_1', if it is

less than ε, then the S'_1 mesh in the cube is displayed with red color; otherwise, it is displayed with gray color. The results are shown in Figure 19 (a) and (c). Since the isosurface segmentation diagram in Figure 17 shows that isosurface S'_1 is only formed by two types of boundaries: the air and medium value material boundary and the air and high value material boundary. Therefore, the gray portion of S'_1 corresponds to the air and medium value material boundary. The same method is applied to segment isosurface S'_2 with S'_1 being the reference isosurface. The results are shown in Figure 19 (b) and (d). (e) shows a combined rendering with both S'_1 and S'_2.

A rendering of the engine dataset using the direct volume rendering technique based on a 2D opacity function is given in [Kin99]. It is shown in Figure 19 (f). This rendering shows only the boundary between the engine's high value material and air, which helps the user learn structural information about the dataset. Comparing this direct volume rendering, the isosurface segmentation renderings of the dataset are clearer and have less noise. In addition, they can be used for further modeling since they contain triangular meshes.

The results of testing the segmentation method with the tooth dataset are shown in Figure 20. The tooth dataset is more complex than the engine dataset since it has four major materials. Also, as shown in the isosurface segmentation diagram in (a), the isosurface with isovalue 601, S'_3, is formed by three different types of boundaries: the background-dentin, the background-enamel, and pulp-dentin boundaries. To separate these three types of boundaries, two reference isosurfaces are used. They are the isosurface with isovalue 288, S'_4, and the isosurface with isovalue 954, S'_5. If at a cube K that interests with S'_3, the distance of S'_3 to S'_4 is smaller than a given threshold, then S'_3 in K belongs to the pulp-dentin boundary; otherwise, the distance of S'_3 to S'_5 is checked and if this distance is smaller than a given threshold, S'_3 in K belongs to the background-enamel boundary, if not, it belongs to the background-dentin boundary. The results of segmenting S'_3 is demonstrated in (e). If only the isosurface mesh for one type of boundary is displayed, that boundary can be displayed separately from other features. This is shown in (f), (g), and (h). This method successfully separates the three types of boundaries of S'_3, which is hard to be achieved by many other methods. The segmentation of S'_5 is shown in (b), (c), and (d). A combined rendering with both S'_3 and S'_5 is given in (i).

This method can also be used to separate an isosurface that passes through the material interior. Figure 21 gives such an example with the tooth dataset. In this example, isovalue 838, S'_6, is in the dentin data value range. However, 838 is also in between the data values of the background (at about 390) and the enamel (at about 1200). Thus, S'_6 crosses both the interior of the dentin and the background-enamel boundary. To separate these two different features, the isosurface with isovalue 954 is used as the reference isosurface. (a) shows a regular rendering of isosurface S'_6. (b) shows the segmentation of the isosurface. The separated features are shown in (c) and (d).

For the engine dataset, it takes 0.81 seconds to segment and render the isosurface with isovalue 184, which is shown in Figure 19 (b); while without segmentation, rendering itself takes 0.48 seconds. Segmenting and rendering the isosurface with isovalue 78 shown in Figure 19 (a) takes 2.75 seconds, while rendering only takes 0.69 seconds. For the tooth dataset, segmenting and rendering the isosurface with isovalue 601 shown in Figure 20 (e) takes 1.28 seconds; while rendering without segmentation takes 0.32 seconds.

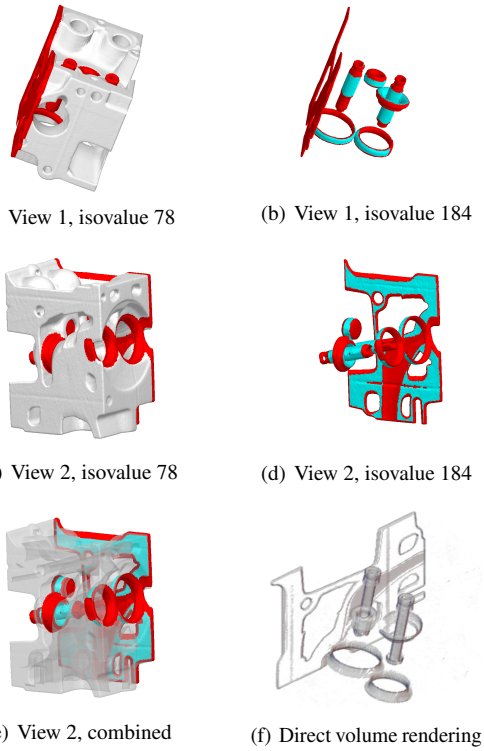

(a) View 1, isovalue 78 (b) View 1, isovalue 184

(c) View 2, isovalue 78 (d) View 2, isovalue 184

(e) View 2, combined (f) Direct volume rendering

Figure 19: *Isosurface segmentation results for the engine dataset, which are demonstrated in two views. In (a) and (c), the isosurface with isovalue 78 is displayed. Here, the high value material's boundary with air is shown in red, and the medium value material's boundary with air is shown in gray. In (b) and (d), the isosurface with isovalue 184 is shown with the air and high value material boundary shown in red, and the medium value material and high value material boundary shown in cyan. A combined rendering with both isosurfaces is given in (e). A direct volume rendering of the dataset that only shows the air and high value material boundary (adapted from [Kin99]) is given in (f).*

5. Conclusion and Future Work

This paper proposed two new isosurface measures. One is used for detecting representative isovalues and one is used for isosurface segmentation. Both achieve good results when tested with real datasets. In the future, research work may be conducted to discover the relationship between the VOA measure and the thickness of the material boundary, and utilize the VOA measure in designing the transfer functions for direct volume rendering. Future research work may also result in a pure analytical method to compute interval volumes, which can be both fast and accurate. It can greatly reduce the execution time of computing the VOA measure.

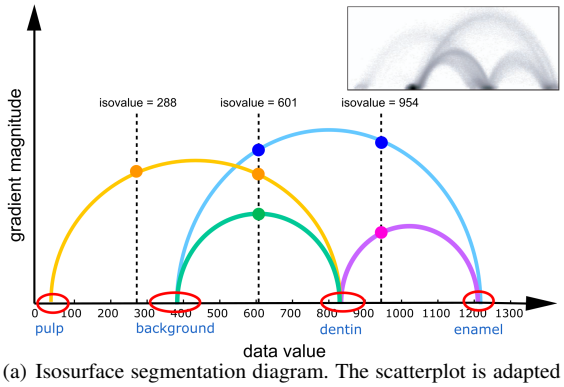

(a) Isosurface segmentation diagram. The scatterplot is adapted from [KKH02].

(b) Isovalue 954 (c) Background-enamel (d) Dentin-enamel

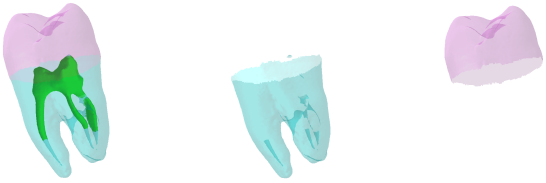

(e) Isovalue 601 (f) Background-dentin (g) Background-enamel

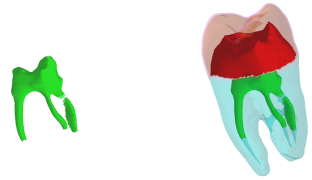

(h) Pulp-dentin (i) Combined

Figure 20: *Isosurface segmentation for the tooth dataset. (a) Isosurface segmentation diagram. (b) Segmented isosurface with isovalue 954. The two portions of this isosurface that correspond to the background-enamel and background-dentin boundaries are shown in (c) and (d), respectively. (e) Segmented isosurface with isovalue 601. This isosurface contains the background-dentin boundary in (f), the background-enamel boundary in (g), and the pulp-dentin boundary in (h). A combined rendering using both isosurfaces is shown in (i).*

(a) Regular rendering (b) Segmented isosurface

(c) Dentin-enamel (d) Dentin

Figure 21: *Segmented isosurface with isovalue 838 of the tooth dataset.*

References

[BM10] BRUCKNER S., MÖLLER T.: Isosurface similarity maps. *Computer Graphics Forum 29*, 3 (2010), 773–782. 2

[DCM13] DUFFY B., CARR H., MÖLLER T.: Integrating isosurface statistics and histograms. *IEEE Trans. on Visualization and Comp. Graphics 19*, 2 (2013), 263–277. 2, 3, 4

[FMS95] FUJISHIRO I., MAEDA Y., SATO H.: Interval volume: A solid fitting technique for volumetric data display and analysis. In *Proceedings of Visualization '95* (Atlanta, USA, 1995), pp. 151–158. 1

[Guo95] GUO B.: Interval set: A volume rendering technique generalizing isosurface extraction. In *Proceedings of Visualization '95* (Atlanta, USA, 1995), pp. 3–10. 1

[Kin99] KINDLMANN G.: *Semi-Automatic Generation of Transfer Functions for Direct Volume Rendering*. Master's thesis, Cornell University, USA, 1999. 2, 4, 9, 10

[KKH02] KNISS J. M., KINDLMANN G. L., HANSEN C. D.: Multidimensional transfer functions for interactive volume rendering. *IEEE Trans. Vis. Comput. Graph. 8* (2002), 270–285. 2, 11

[Kni02] KNISS J. M.: *Interactive volume rendering techniques*. Master's thesis, University of Utah, USA, 2002. 1

[KW10] KHOURY M., WENGER R.: On the fractal dimension of isosurfaces. *IEEE Trans. on Visualization and Comp. Graphics 16*, 6 (2010), 1198–1205. 2

[LC87] LORENSEN W. E., CLINE H. E.: Marching cubes: A high resolution 3D surface construction algorithm. *SIGGRAPH Computer Graphics 21*, 4 (Aug. 1987), 163–169. doi:10.1145/37402.37422. 1

[Mor16] MORGAN F.: *Geometric Measure Theory: A Beginner's Guide*. Academic Press, 2016. 3

[MSS94] MONTANI C., SCATENI R., SCOPIGNO R.: Discretized marching cubes. In *Visualization '94* (Washington D.C., 1994), pp. 281–287. 7

[NY06] NEWMAN T., YI H.: A survey of the marching cubes algorithm. *Computers & Graphics 30*, 5 (2006), 854–879. 1

[PWB01] PEKAR V., WIEMKER R., BYSTROV D.: Fast detection of meaningful isosurfaces for volume data visualization. *Proceedings Visualization, 2001. VIS '01.* (2001), 223–230. 2, 3, 4

[SSD*08] SCHEIDEGGER C. E., SCHREINER J. M., DUFFY B., CARR H. A., SILVA C. T.: Revisiting histograms and isosurface statistics. *IEEE Transactions on Visualization and Computer Graphics 14* (2008). 2, 3, 4

[TLM01] TENGINAKAI S., LEE J., MACHIRAJU R.: Salient iso-surface detection with model-independent statistical signatures. *Proceedings Visualization, 2001. VIS '01.* (2001), 231–238. 2

[Wan19] WANG C.: Accurate computation of interval volume measures for improving histograms. In *Proceedings of 14th International Symposium on Visual Computing (ISVC '19)* (Lake Tahoe, NV/CA, USA, 2019), pp. 315–329. 2, 3

[Wen13] WENGER R.: *Isosurfaces: geometry, topology, and algorithms*. CRC Press, 2013. 1, 2, 4